JOURNAL OF GEOPHYSICAL RESEARCH, VOL. 114, B10306, doi:10.1029/2008JB005939, 2009

Anatomy of a seismoelectric conversion: Measurements and conceptual modeling in boreholes penetrating a sandy aquifer

J. C. Dupuis,[1,2] K. E. Butler,[1] A. W. Kepic,[2] and B. D. Harris[2]

Received 17 July 2008; revised 25 June 2009; accepted 13 July 2009; published 3 October 2009.

[1] Conversions of compressional seismic waves to electric fields have been measured in two boreholes drilled in an unconfined sandy aquifer on the Gnangara Mound near Perth, Australia. The seismoelectric conversions at both field sites occurred in the vicinity of the water table at 13-m depth and yielded maximum amplitudes of 1 μV/m using a sledgehammer source on surface. Partially cemented layers, inferred from geological and geophysical logs, straddle the water table and may play a role in generating the conversion and influencing its amplitude distribution. The dense vertical sampling used in these borehole experiments reveals spatial and temporal polarity reversals of the interfacial signal which provide new evidence in support of the conceptual model for seismoelectric conversions at interfaces. We demonstrate that the growth rate of the source zone and its maximum vertical extent below the water table are encoded in the polarity of the interfacial signal. These experiments confirm that vertical seismoelectric profiling can be used to gain further insight into seismoelectric conversions and characteristics of interfaces that makes them amenable to detection.

Citation: Dupuis, J. C., K. E. Butler, A. W. Kepic, and B. D. Harris (2009), Anatomy of a seismoelectric conversion: Measurements and conceptual modeling in boreholes penetrating a sandy aquifer, *J. Geophys. Res.*, *114*, B10306, doi:10.1029/2008JB005939.

1. Introduction

[2] Electrokinetic coupling between seismic waves and electrical fields has attracted significant attention over the last 15 years because of its expected sensitivity to pore fluid properties and fluid flow permeability. There is particular interest in using the phenomenon to image subsurface interfaces, combining the resolution of seismic methods with material property sensitivities more akin to those of electrical methods. While theoretical models, numerical simulations, and recent laboratory measurements [*Zhu et al.*, 2008; *Bordes et al.*, 2006, 2008] have contributed to expand our understanding of seismoelectric effects, there remains a need for convincing field measurements that can be used to evaluate the models and identify the types of interfaces most amenable to detection.

[3] *Dupuis et al.* [2007] recently measured remarkably clear seismoelectric conversions from shallow interfaces within a sandy aquifer on the Gnangara Mound near Perth, Australia. A surface survey, conducted along a 300-m traverse imaged two distinct interfaces interpreted as a water retentive layer and the base of the vadose zone at depths up to 15 m. In this paper we concentrate on the origin of interfacial signals in the Gnangara Mound area by presenting the results of measurements made in boreholes. The borehole experiments provide insight into the nature of interfacial seismoelectric conversions and suggest that the physical contrasts responsible for seismoelectric conversion at the base of the vadose zone, or water table, may include partial cementation in addition to changes in water saturation and electrical conductivity as previously assumed [*Dupuis et al.*, 2007].

[4] Electrokinetic coupling arises from the flow or oscillation of ions in the electric double layer that forms between the pore fluid and the solid grains in rocks or soils. Two different types of electrokinetic seismoelectric signals can be generated by compressional seismic waves. The first is termed coseismic because it is local to the seismic wave and is observed in homogeneous media as a result of charge separation between zones of compression and dilatation associated with the seismic wave [*Neev and Yeatts*, 1989; *Pride and Haartsen*, 1996]. The second is termed an interfacial signal because it is generated at an interface where the symmetry of the charge distribution within the seismic wave is altered. The resulting electric field radiates away from the interface at the speed of an electromagnetic wave and exhibits amplitude variations similar to that of an electric dipole positioned at the heterogeneity directly under the seismic source [*Thompson and Gist*, 1993; *Butler et al.*, 1996; *Haartsen and Pride*, 1997; *Garambois and Dietrich*, 2002; *Dupuis et al.*, 2007].

[5] Other poroelastic wave types such as shear waves [*Bordes et al.*, 2006, 2008], and Stoneley waves in boreholes [*Mikhailov et al.*, 2000; *Hunt and Worthington*, 2000; *Singer et al.*, 2006] can generate seismoelectric or seismomagnetic signals but the compressional wave (P wave) has

[1]Department of Geology, University of New Brunswick, Fredericton, New Brunswick, Canada.
[2]Department of Exploration Geophysics, Curtin University of Technology, Perth, Western Australia, Australia.

0148-0227/09/2008JB005939$09.00

generally received the most attention in field experiments [*Martner and Sparks*, 1959; *Thompson and Gist*, 1993; *Butler et al.*, 1996; *Mikhailov et al.*, 1997; *Russell et al.*, 1997; *Beamish*, 1999; *Butler et al.*, 1999; *Garambois and Dietrich*, 2001; *Dupuis and Butler*, 2006; *Kulessa et al.*, 2006; *Dupuis et al.*, 2007; *Haines et al.*, 2007; *Strahser et al.*, 2007]. It is favored because models predict that it has the best potential to generate interfacial signals of sufficient strength to be observed on surface and used to map heterogeneities [*Haartsen and Pride*, 1997; *Garambois and Dietrich*, 2002; *Pride and Garambois*, 2002, 2005]. However, the measurement of these weak interfacial signals under field conditions is challenging, particularly on surface where both ambient environmental noise and coseismic arrivals tend to cause the most interference.

[6] The geometry of a vertical seismoelectric profiling (VSEP) survey, as described by *Dupuis and Butler* [2006], provides several benefits over surface-based field measurements and helps to increase the signal-to-noise ratio of the measurements. First, since the measurements are made in situ they are made closer to the seismoelectric source and thus should have larger amplitudes. Second, since the receivers are immersed in the borehole fluid they have lower contact impedance and are more immune against electromagnetic interference. Finally, this geometry also allows for the separation of the interfacial seismoelectric signal from the coseismic signal associated with the direct arrival. This separation is achieved by placing the receivers below an interface so that interfacial signals reach the receivers before the coseismic arrivals.

[7] *Martner and Sparks* [1959], *Butler et al.* [1996], and *Russell et al.* [1997] all used boreholes for the signal separation they can provide. Shots were fired at varying depths and interfacial signals were measured at surface before the arrival of the seismic wave. *Martner and Sparks* [1959] also performed a second experiment in which explosives were detonated in deep shot holes while the seismoelectric signals were measured by a single electrode referenced to the surface. This experiment revealed an interfacial signal, which was generated when the P wave reached the base of the weathered layer. Additional interesting borehole experiments have been reported by *Hunt and Worthington* [2000] and *Mikhailov et al.* [2000] but these were performed using Stoneley/tube waves in fractured rock while the current work studies seismoelectric signals associated with P waves in unconsolidated sediments.

[8] In addition to establishing the ability of seismoelectric methods to detect partially cemented layers within unconsolidated sediments, the borehole measurements presented here show the evolution of an interfacial signal as it is generated. The polarity and amplitude characteristics of the measured interfacial signals are found to be consistent with the predictions of a conceptual bipole-like model for the seismoelectric source. The measurements also represent a unique data set that may be used in the future to fuel further development of numerical modeling codes.

2. Field Experiments

2.1. Site Description

[9] The VSEP experiments were performed in August and September, 2006 on the Gnangara Mound, which is an important water recharge and storage area for Perth, Western Australia [*Salama et al.*, 2005]. Two PVC-cased boreholes, P220 and GG1(O), were chosen because of their long slotted intervals (allowing galvanic contact between the electrodes and the formation) and their relatively simple geology. The map in Figure 1 locates these two boreholes as well as the location of the seismoelectric traverse of *Dupuis et al.* [2007], labeled P-90 on the map. The surficial sediments at P220 and GG1(O) have very different characteristics that affects the land use at these field sites [*Salama et al.*, 2005].

[10] Borehole P220 is located within a pine plantation in a region where the surficial geology consists of sands derived from weathering/leaching of Tamala Limestone, a calcareous wind blown deposit composed of varying proportions of quartz sands, fine to medium grained shell fragments and clayey lenses [*Davidson*, 1995]. The driller's log for this borehole reports unconsolidated fine light colored sands to a depth of 50 m which suggest that the Tamala Limestone at this site has been significantly weathered over time. *Davidson* [1995] reported that the quartz sands in this formation are predominantly medium grained and moderately sorted and commonly stained with limonite. The water table depth in this bore remained at 12.65 m during the period when all measurements were made.

[11] GG1(O) is located within native bush land where the surficial geology is composed of Bassendean sands. *Davidson* [1995] indicated that the quartz sands found in this region are moderately sorted and commonly have an upward fining progression in grain size. He also reports that a layer of friable, limonite-cemented sand, colloquially called "coffee rock", occurs throughout most of the area near the water table. The water table depth in this bore remained at 13.00 m during the period when all the measurements were made.

[12] The surficial geology near borehole P-90, where the seismoelectric traverse was acquired [*Dupuis et al.*, 2007], is similar to that at GG1(O) although the ground cover included native bush on one side of the survey line and a pine plantation on the other.

2.2. Vertical Seismic and Seismoelectric Profiles

[13] The VSEPs were acquired by lowering a multielectrode array down a slotted, PVC-cased borehole and striking a sledgehammer seismic source on surface, offset 3.5 m from the borehole collar. The electrodes were made of tinned copper wire wrapped around segments of PVC pipe that were 10 cm long and 2.5 cm in diameter. Seven electrodes, spaced two meters apart, were connected to a 36-m multipaired cable and the connections were waterproofed with a urethane compound. The measurements reported in this paper were made by pairing the electrodes so as to give six dipoles each 2 m in length as shown in Figure 2.

[14] The signals from the dipoles were buffered at surface using custom-built differential preamplifiers which provided a gain of 10, and were digitized using a 24-bit seismograph (Geometrics Geode) with a sample rate of 62.5 μs. The electrode array was raised in 25 cm increments and 20 sledgehammer blows were recorded at every depth, thereby providing a maximum fold of 120 shots at each depth (taking into consideration the redundancy provided by

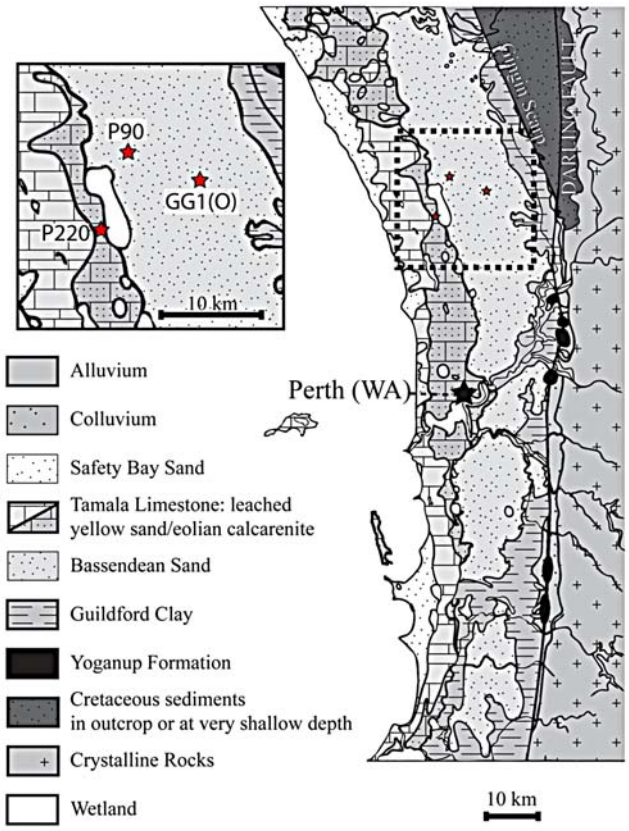

Figure 1. Location of boreholes used in this study, P220 and GG1(O), and the location of the seismoelectric imaging experiment of *Dupuis et al.* [2007] labeled P-90. This map is an adaptation from the surficial geology map of *Davidson* [1995].

6 dipoles). All shots were acquired and processed individually for harmonic noise removal [*Butler and Russell*, 2003] so that records exhibiting large amounts of residual noise could be omitted from the stacks. Typical powerline noise levels were relatively low at 0.1 to 5 μV/m. On average, the number of traces rejected at each depth was less than 2%.

[15] Vertical seismic profiles (VSPs) were also acquired at each site. A hydrophone was lowered to the bottom of the boreholes and raised in 25 cm increments until it reached the water table. As in the VSEP survey, the shot point was located on surface 3.5 m from the borehole casing. Because of the high sensitivity of the hydrophone, a lighter hammer was used as a source and only two shots were required to obtain sufficient signal-to-noise ratio. A second VSP was acquired at P220 with a wall-locking borehole geophone and a sledgehammer source in order to obtain a velocity profile for the vadose zone above the water table.

3. Results and Discussion

[16] The VSP and VSEP data for borehole P220 are displayed in Figures 3a and 3b. The VSP exhibits direct P-wave arrivals (A) followed by lower velocity and lower frequency tube waves. The pressure associated with the direct P-wave arrivals at P220 varied from a maximum of 50 μbars, near the water table, to 20 μbars at the bottom of the profile. The VSEP is more complex as several wave modes, absent from the VSP, interfere with one another. The most interesting signal for the purpose of this work is the event labeled (B) that is generated at approximately 26.25 ms and shows both polarity and amplitude variations with depth. The signal arrives essentially simultaneously at all the receivers irrespective of their depth and precedes the arrival of any seismic waves at depth. These characteristics are expected of a seismoelectric conversion measured below the interface where it is generated. The maximum peak amplitude of the interfacial signal is approximately 1 μV/m and is observed at 20.25-m depth.

[17] The VSP and VSEP data acquired in the second borehole, GG1(O), are displayed in Figures 4a and 4b. The direct P-wave arrivals in the hydrophone VSP are labeled (A) and had amplitudes varying from 30 to 5 μbars. As was done for P220, the times of the direct arrivals are transferred onto the VSEP. The direct (coseismic) arrivals in this borehole are much easier to observe and it is evident that their amplitudes vary with depth which is similar to the results of *Dupuis and Butler* [2006]. The maximum amplitude of the coseismic signal, 6 μV/m, occurs between 19 and 21 m. The interfacial signal, labeled (B) on Figure 4b, shows similar characteristics as the one measured at P220 (i.e., simultaneous arrival at receivers irrespective of their depth and polarity variations with depth) but is much more subtle, decaying rapidly with depth. Thus while the interfacial signal at P220 is observed over more than 14-m

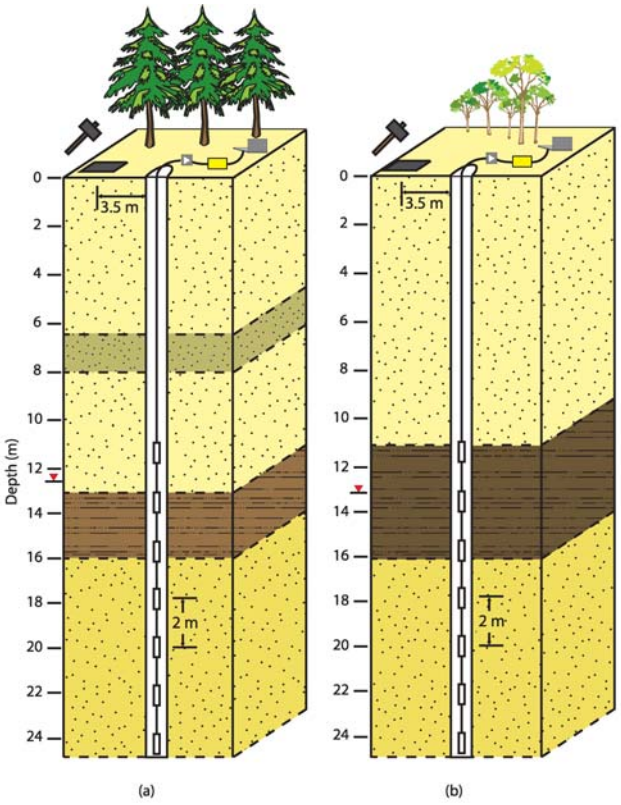

Figure 2. Experimental setup for vertical seismoelectric profiling at borehole (a) P220 and (b) GG1(O). Inferred interfaces from the geophysical logs are indicated by dashed lines. The darker areas represent inferred partially cemented layers.

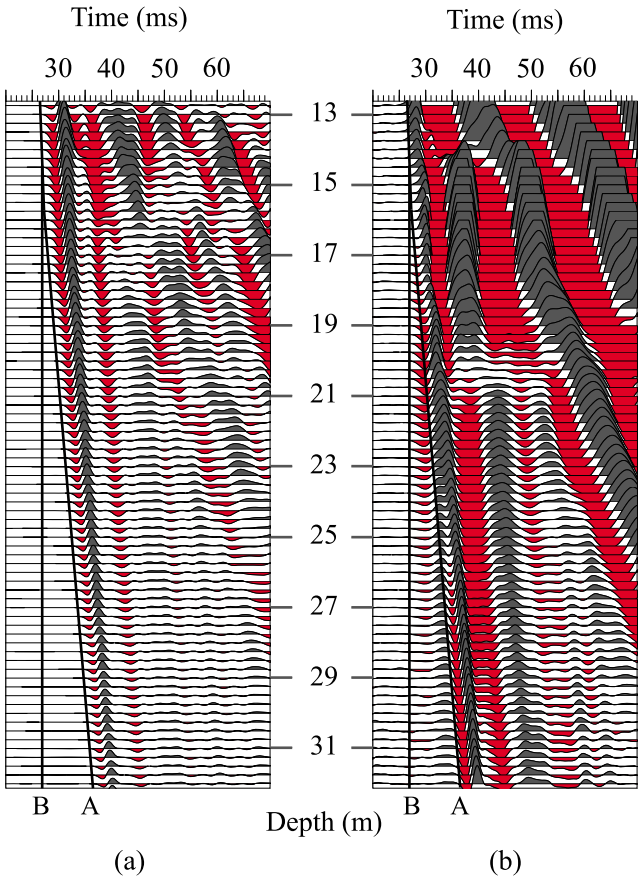

Figure 3. (a) Vertical seismic and (b) seismoelectric profiles for borehole P220. A Butterworth bandpass filter (60–500 Hz) has been applied to both data sets and traces are plotted at true relative amplitudes.

depth, the interfacial signal observed in GG1(O) is only evident over approximately ≈2.5 m (i.e., 14.75 to 17 m). Close scrutiny of the arrival times over this short interval reveals a small trigger uncertainty of the order of about two tenths of a millisecond which is imposed by instrumentation limitation. This trigger uncertainty, however, does not detract from simultaneity of the interfacial signal observed at GG1(O).

3.1. Origin of the Interfacial Signal

3.1.1. Borehole P220

[18] In order to identify the interfaces that generate the seismoelectric conversions we examine the velocity model derived from the VSP surveys, induction-conductivity and gamma-ray logs acquired in 2006 surveys, and the simple geological logs taken when the boreholes were drilled, more than 30 years ago.

[19] The elevated electrical conductivity and gamma ray counts observed between 6- and 8-m depth in borehole P220 (Figures 5a and 5b) are suggestive of a layer with elevated clay content. Moving down the hole, an abrupt increase in conductivity from about 6 to 60 mS/m is observed on crossing the water table which was measured in the hole at a depth of 12.65 m. A closer inspection of the gamma log reveals a small drop in gamma ray emissions for a region starting just above the water table (≈12.2 m) and extending down to 16-m depth. The P-wave velocity model (Figure 5c) derived from first arrival times in the hydrophone and borehole geophone VSPs show an elevated P-wave velocity of 3000 m/s between 13- and 16-m depth. This is well above the more usual range of 1500–2000 m/s expected for water-saturated sands, suggesting that the region is partially cemented.

[20] The onset of the interfacial signal at 26.25 ms (Figure 3b) corresponds to the arrival of the P wave at the water table. It is to be expected, therefore, that the interfacial signal observed at P220 is related to two important variations in porous media properties: (1) a sharp increase in conductivity caused by a conductive pore fluid, and (2) a strong impedance contrast from the water table and the coincident partially cemented layer.

3.1.2. Borehole GG1(O)

[21] Figure 6 presents the conductivity and gamma ray logs and the P-wave velocity profile for borehole GG1(O). The gamma emissions and conductivity values throughout the upper 11 m of this hole are lower than those measured at P220 which indicates that the sands at this site contain very little clay and therefore may have less water retention capabilities than the sands at P220. The abrupt increase in conductivity observed at 13.00 m corresponds with the water table in this hole. The increase in the gamma log response at approximately 11-m depth correlates with a layer of brown sand and black sandstone reported in the

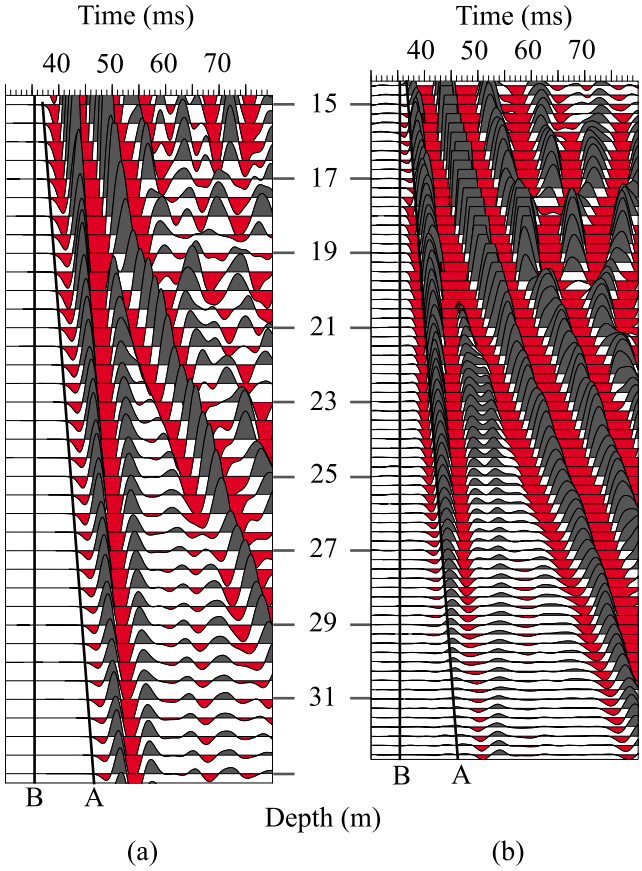

Figure 4. (a) Vertical seismic and (b) seismoelectric profiles acquired for borehole GG1(O). A Butterworth bandpass filter (120–300 Hz) has been applied to both data sets and traces are plotted at true relative amplitudes.

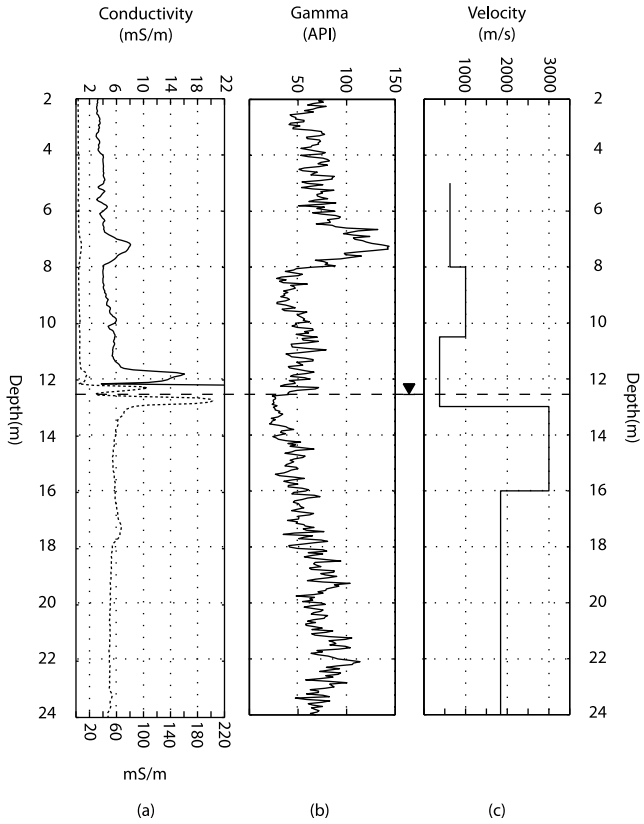

Figure 5. (a) Conductivity and (b) gamma-ray logs acquired in borehole P220 penetrating leached Tamala Limestone. The velocity profile (c) is derived from the direct P-wave arrivals from a VSP acquired using a borehole geophone.

driller's log that probably corresponds to the limonite-cemented sands (coffee rock) reported by *Davidson* [1995]. The P-wave velocity log, derived from the hydrophone VSP, shows a velocity of 2800 m/s for a region that spans from the water table to 20-m depth. Since only hydrophone data is available, the VSP at GG1(O) cannot provide information on the extent of this partially cemented layer above the water table. We expect, however, that the top of the cemented layer corresponds with the brown sand and black sandstone (and the elevated gamma ray response) reported at 11-m depth.

[22] The compressional wave reaches the top of the water table in borehole GG1(O) at 36 ms, approximately 1 ms after the onset of the interfacial signal in Figure 4b. If the velocity of the partially cemented layer remains constant above the water table, the 1 ms difference would place the origin of the interfacial signal at the top of the partially cemented layer at $\approx$11 m.

3.2. Polarity of the Interfacial Signal

3.2.1. Conceptual Model

[23] The polarity reversal of the interfacial signal measured in borehole P220 encodes important information about the spatial and temporal evolution of the seismoelectric source. To demonstrate, we begin this section with a simple conceptual model.

[24] The diagram in Figure 7 represents a simplified conceptual model of the electric charge distribution and resulting electric fields comprising the seismoelectric conversion generated by a P-wave reflecting at a perfect reflector [*Butler et al.*, 1996]. The assumption of a perfect reflector is a reasonable first-order approximation in this case because of the large acoustic impedance contrast that exists between the unsaturated sediments and the saturated, partially cemented layer. However, abrupt changes in the mechanical and/or electrical characteristics of a porous medium, such as electrical conductivity, zeta potential, porosity and permeability are also expected to alter the charge distribution and give rise to interfacial signals [*Haartsen and Pride*, 1997; *Garambois and Dietrich*, 2002]. The diagram in Figure 7a schematically depicts the instant in time where the first seismic Fresnel zone for this reflector has formed. Thus the lateral extent of this lens-shaped zone is the Fresnel radius while the vertical extent is the dominant wavelength of the seismic P-wave in the top material. This instant in time is important because according to *Thompson and Gist* [1993] and *Garambois and Dietrich* [2002] the interfacial signal is expected to reach its maximum (at least in the far-field) once the first Fresnel zone has taken shape.

[25] The dipoles used as receivers in the borehole are short (2 m long) in comparison to the height of the source zone which contributes to the signal. So it is possible to measure the potential differences at points inside and outside this zone. Receivers placed above and below the

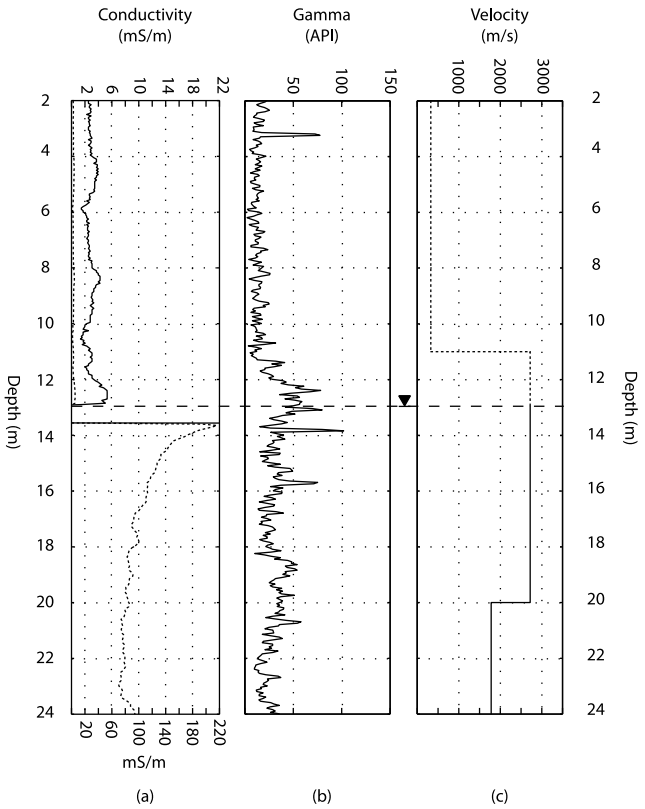

Figure 6. (a) Conductivity and (b) gamma-ray logs acquired in borehole GG1(O) penetrating Bassendean Sands. The velocity profile (c) is derived from the direct P-wave arrivals from a VSP acquired using a hydrophone.

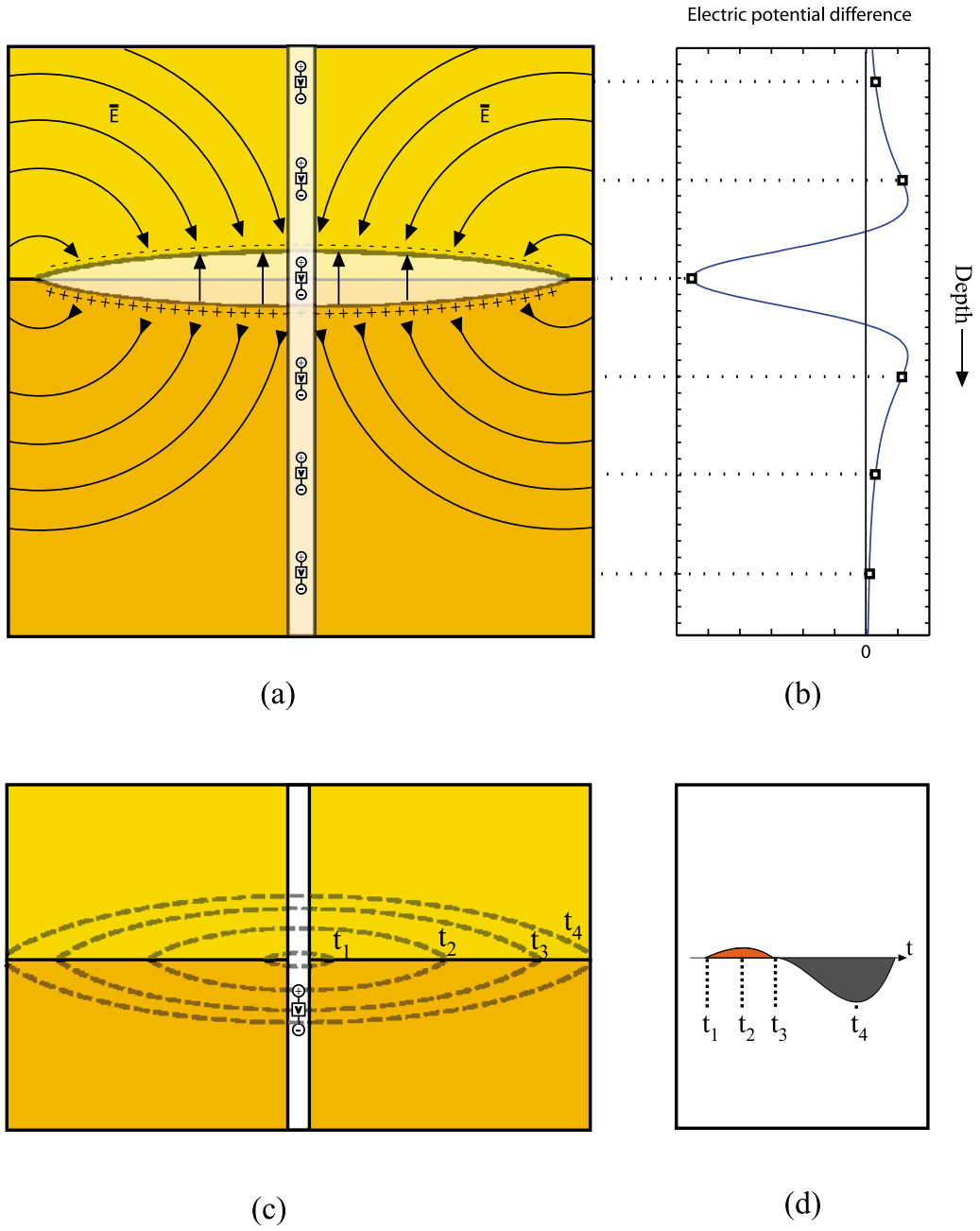

Figure 7. (a) Schematic representation of the conceptual charge distribution obtained at a perfect reflector interface. (b) Electric potential measured by the measurement dipoles. (c) Schematic representation of the polarity effects caused by an expanding source region and (d) expected electric potential difference measured at the receiver.

source zone will record positive potential differences since the field lines are directed downward (the lower electrode is used as the reference or negative electrode in each of our dipole pairs). On the other hand, dipoles located within the source region will sense upward electric fields and will record negative potential difference as illustrated in Figure 7b. From this model, the transition from negative to positive should occur once the mid point of the receiver dipole goes to a depth $\lambda/2$ beyond the generating interface (where λ is the dominant wavelength of the seismic P wave in the top material).

[26] Apart from the abovementioned change in polarity with receiver depths, some receivers will also experience a change in signal polarity with time. To understand this concept, let us consider a receiver positioned below the interface as in Figure 7c. At time t_1 the receiver will measure a small positive potential difference because it is outside the zone where the interfacial signal is being generated. As the source zone moves toward the positive electrode of the receiver, the potential difference measured at the receiver will increase. After reaching a maximum at time t_2, the potential difference will start to decrease until the electric fields inside and outside the active zone cancel each other (t_3). As the source continues to expand, leaving the receiver dipole completely inside, the receiver will measure negative potential differences (t_4). This evolution

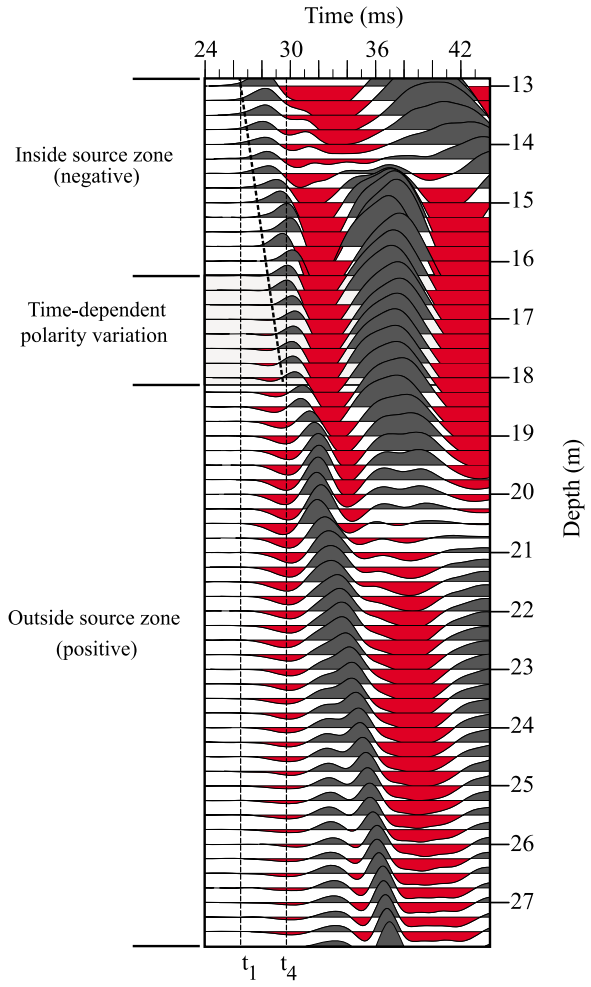

Figure 8. Enlarged portion of the P220 VSEP that shows the two type of polarity reversal measured in a borehole and the three regions that exist for an interfacial signal measured in situ. Traces are plotted at their true relative amplitudes.

of signal polarity with time can be seen in the VSEP for borehole P220 for traces between 16.5- and 18.0-m depth as shown in Figure 8. The polarity inversion over this transition interval causes the measured interfacial signal to have a higher-frequency content than the signal measured outside the transition zone.

3.2.2. Deciphering the Polarity Information

[27] The information encoded in the polarity transitions observed over both time and depth at P220 can be used to determine the rate at which the source zone takes shape and the maximum vertical extent it reaches. We begin this analysis by identifying the known quantities obtained from the VSEP and the VSP.

[28] The first observation that can be made is that the onset of the interfacial signal (labeled t_1 on Figure 8) coincides closely with the 26.25 ms arrival time of the P wave at the water table (12.65 m). According to the velocity profile of Figure 5c, however, the physical property contrast in this region is not only caused by water saturation but is also a consequence of partial cementation between 13- and 16-m depth. We cannot be sure whether it is the change in water saturation (and resulting change in conductivity) or the change in cementation that dominates in producing the interfacial signal since arrival times would differ by only 0.1 ms. We therefore assume that the interfacial signal is caused by a combination of the large acoustic impedance of the cemented layer and the large increase in conductivity at the water table. We also assume, for purpose of the modeling that follows, that the top of the cemented layer and the water table are coincident.

[29] The second observation necessary for this analysis can be made by considering the time at which the interfacial signal reaches its maximum amplitude, which is labeled t_4 in Figure 8. At this instant in time (29.75 ms), the source zone has reached its maximum vertical extent. According to our model, the base of the source zone should be found at the depth where the polarity switches along line t_4 in Figure 8. Following this line, we can observe the polarity of the signal flipping from negative to positive in the interval between 18 and 18.25 m which means that that the bottom of the source zone probably lies in this interval.

[30] The last necessary piece of information is obtained by considering the higher-frequency signal in the transition zone where the polarity switches from positive to negative during development of the seismoelectric source. In this transition zone, the polarity of the signal at a given depth changes with time as the source zone expands beyond the midpoint of the dipole receiver at that depth. Fitting a line through the points where the transition occurs gives the velocity at which the source zone is expanding ($\approx$1500 m/s) which is comparable to the P-wave velocity in the saturated sediments measured from the first break arrivals of the VSP below the partially cemented layer (1780 m/s). If we use this line to project back to t_1, as is done in Figure 8 we get a confirmation that the signal originated from a depth of approximately 13 m.

3.3. Conceptual Modeling the Interfacial Signal

3.3.1. Simple Bipole Model

[31] The source region for the interfacial signal of the conceptual model presented in section 3.2 can be described by using charged spherical caps [*Butler et al.*, 1996] which in turn can be modeled by a multipole expansion. Numerical results [*Garambois and Dietrich*, 2002] have shown that the dipole term dominates the multipole expansion when interfaces are deeper than a few wavelengths and it has therefore become common to compare the amplitude versus offset characteristics of numerical simulations and field measurements to those of a short electric dipole positioned at the interface beneath the seismic source.

[32] In this case however, the far-field dipole model is inappropriate because the measurements are made in the near field of the source. We therefore propose to decompose the dipole into a positive and negative point charge to form a bipole with a charge strength chosen to best fit measured data. The suitability of a bipole source to model an interfacial signal measured in a borehole is demonstrated below.

[33] The bipole at the water table starts to take shape once the symmetry of the coseismic field is broken at 26.25 ms. We know from the data that the charged front of the source zone, represented here by a positive charge, moves at a velocity of 1500 m/s in the downward direction. The rate of expansion of the source zone above the water table cannot be constrained by the VSEP data, but we can assume that it is slower, in keeping with the slower P-wave velocity of

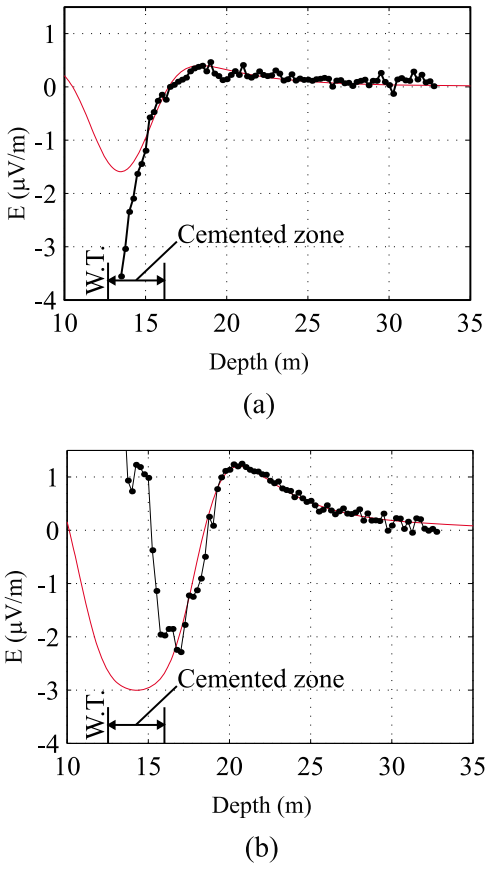

Figure 9. Potential differences normalized by dipole length (2 m) versus depth for interfacial signal measured (dots) and modeled (solid line) in the VSEP experiment at P220 at (a) 28.0 and (b) 29.75 ms. The modeled bipole is positioned directly below the shot point (3.5 m from the borehole) and pole separation is determined by the instant in time and the expansion rate of the source zone. The water table level is indicated by W.T.

unsaturated sediments. In this model, we assume that the negative charged front, represented here by a negative point charge, is moving toward surface with a velocity of 560 m/s which represents the average P-wave velocity in the unsaturated sediments obtained from the VSP.

[34] The VSEP data provides us with the opportunity to study how the amplitude of the signal varies with depth at any instant in time. We choose two discrete instants to compare measured amplitude distributions to those predicted by a bipole model. The first is at 28 ms, which is the halfway mark between the times of signal onset and maximum development and the second is at 29.75 ms, when the source zone has reached its maximum size. Observed amplitude variations with depth are compared to the predictions of the bipole model for those two instants in time in Figure 9. We can see that the bipole model provides a good fit to the data below the water table at both instants in time and that the shift of the peak amplitude to greater depth over time corresponds well to the shift associated with the expansion of the source zone. The fit of the model, however, is not as good in the region immediately below the water table interface. This is in part because of a lack of information on the rate of expansion of the source zone above the water table and because of the interference with the coseismic arrival at these depths.

3.3.2. Importance of the Conductivity Structure

[35] It is not possible to do the same type of signal analysis on the interfacial signal observed at GG1(O) because it is only evident on a very limited number of traces. We attribute this to the different conductivity structures evident in the induction logs (Figures 5a and 6a) from boreholes P220 and GG1(O). In both boreholes the conductivity log exhibits a high-amplitude oscillation where it crosses the water table. This is interpreted as an artifact of the induction tool's response to an abrupt and large change in conductivity. In borehole P220 (Figure 5a) this artifact extends approximately 1 m below the water table, below which the conductivity log exhibits a stable reading of approximately 60 mS/m. The extent of the artifact in borehole GG1(O) should be the same as both holes were logged upward with the same tool and logging speed. It is clear, therefore, by comparison of the logs in Figures 5a and 6a that formation conductivities in the upper part of the saturated zone are two to three times higher in borehole GG1(O), dropping gradually from a high of 180 mS/m at a depth of 1 m below the water table to a background value of 80 mS/m 6 m below the water table. These elevated conductivities are expected to limit the depth of penetration of the interfacial seismoelectric for two reasons: one being that electric fields amplitudes will vary inversely with formation conductivity and the second being that the electric field pattern will remain more concentrated in the high-conductivity zone within a few meters of the water table. It is also possible that the ζ potential was lower at GG1(O) because of an increase in electrolyte concentration which lowers the ζ potential at the silica surface [*Revil et al.*, 1999].

[36] From the driller's logs and geophysical logs (Figures 5 and 6), we suspect that the sources of cementation at the two test sites are different. The brown sand and black sandstone reported at GG1(O) is most likely the coffee rock described by *Davidson* [1995] which he expects to have formed in a shallow marine environment. The origin of the cementation at P220 is unknown and requires further investigation. However, the geological logs make no mention of anomalous conditions, suggesting that the material filling the pore space must have a light color which resembles that of the sand.

4. Conclusions

[37] Results from VSEP experiments, employing a P-wave source at surface and a downhole electrode array, have demonstrated that it is possible for seismoelectric conversions to be measured in a borehole environment where the source-receiver geometry provides separation between interfacial and coseismic signals. The interfacial signals at borehole P220 and GG1(O) were generated in vicinity of the water tables measured in the boreholes. Close examination of the velocity logs revealed partially cemented zones having upper surfaces roughly coincident with the water table. Although geological and geophysical logs indicate that the sources of cementation are different, we expect that these partially cemented layers may play a role in the generation of the interfacial signals by elevating the acoustic impedance of the sediments in addition to the changes in

water saturation and electrical conductivity associated with the water table itself. On the basis of these observations, we hypothesize that the distinct seismoelectric conversion attributed to the base of the vadose zone in the work of *Dupuis et al.* [2007] could be due in part to partial cementation at this interface.

[38] The fact that interfacial signal was measurable over a much larger depth range in one borehole compared to the other is attributed, at least partly, to significant differences in electrical conductivity structure at the two sites. The importance of such electrical screening, and the relative importance of the water table versus partial cementation in generating an interfacial response warrant further investigation, through both field studies and numerical modeling.

[39] The measurements in borehole P220 are unprecedented in exposing the evolution of an interfacial seismoelectric conversion. They reveal spatial and temporal variations in signal polarity and amplitude that may be explained intuitively by considering how relatively short dipole receivers in the borehole would sample the electric field produced by an expanding vertical electric bipole-like source. In that respect, the borehole VSEP measurements support our existing conceptual models for the generation of seismoelectric effects at interfaces. Given that the near-field of the seismoelectric conversion has never been studied up to this point, these measurements provide exciting new information on interfacial signal behavior at an interface that can be used to evaluate current and future full waveform seismoelectric modeling codes.

[40] **Acknowledgments.** Funding for this work was provided by the Water Corporation, the Natural Sciences and Engineering Research Council of Canada (NSERC) Discovery Grant Program, and the Commonwealth Research Centre of Landscapes, Environment, and Mineral Exploration (CRCLEME). Additional funding was provided by the John S. Little Fellowship and an NSERC Postgraduate Scholarship to J.C. Dupuis. We thank Chengchao Xu and Michael Martin of Water Corp. for helping us identify suitable field sites around the Perth region, Paul Wilkes for acquiring geophysical logs, and Dominic Howman for important technical support.

References

Beamish, D. (1999), Characteristics of near-surface electrokinetic coupling, *Geophys. J. Int.*, *137*(1), 231–242, doi:10.1046/j.1365-246x.1999.00785.x.

Bordes, C., L. Jouniaux, M. Dietrich, J. P. Pozzi, and S. Garambois (2006), First laboratory measurements of seismo-magnetic conversions in fluid-filled Fontainebleau sand, *Geophys. Res. Lett.*, *33*, L01302, doi:10.1029/2005GL024582.

Bordes, C., L. Jouniaux, S. Garambois, M. Dietrich, J.-P. Pozzi, and S. Gaffet (2008), Evidence of the theoretically predicted seismo-magnetic conversion, *Geophys. J. Int.*, *174*(2), 489–504, doi:10.1111/j.1365-246X.2008.03828.x.

Butler, K. E., and R. D. Russell (2003), Cancellation of multiple harmonic noise series in geophysical records, *Geophysics*, *68*(3), 1083–1090, doi:10.1190/1.1581080.

Butler, K. E., R. D. Russell, A. W. Kepic, and M. Maxwell (1996), Measurement of the seismoelectric response from a shallow boundary, *Geophysics*, *61*(6), 1769–1778, doi:10.1190/1.1444093.

Butler, K. E., S. W. Fleming, and R. D. Russell (1999), Field test for linearity of seismoelectric conversions, *Can. J. Explor. Geophys.*, *35*(1–2), 20–23.

Davidson, W. A. (1995), Hydrogeology and groundwater resources of the Perth region Western Australia, *Geol. Surv. of West. Aust. Bull. 142*, Geol. Surv. of Western Australia, Perth.

Dupuis, J. C., and K. E. Butler (2006), Vertical seismoelectric profiling in a borehole penetrating glaciofluvial sediments, *Geophys. Res. Lett.*, *33*, L16301, doi:10.1029/2006GL026385.

Dupuis, J. C., K. E. Butler, and A. W. Kepic (2007), Seismoelectric imaging of the vadose zone of a sand aquifer, *Geophysics*, *72*(6), A81–A85, doi:10.1190/1.2773780.

Garambois, S., and M. Dietrich (2001), Seismoelectric wave conversions in porous media: Field measurements and transfer function analysis, *Geophysics*, *66*(5), 1417–1430, doi:10.1190/1.1487087.

Garambois, S., and M. Dietrich (2002), Full waveform numerical simulations of seismoelectromagnetic wave conversions in fluid-saturated stratified porous media, *J. Geophys. Res.*, *107*(B7), 2148, doi:10.1029/2001JB000316.

Haartsen, M. W., and S. Pride (1997), Electroseismic waves from point sources in layered media, *J. Geophys. Res.*, *102*, 24,745–24,769.

Haines, S. S., S. L. Klemperer, and B. Biondi (2007), Seismoelectric imaging of shallow targets, *Geophysics*, *72*(2), G9–G20, doi:10.1190/1.2428267.

Hunt, C. W., and M. H. Worthington (2000), Borehole electrokinetic responses in fracture dominated hydraulically conductive zones, *Geophys. Res. Lett.*, *27*, 1315–1318.

Kulessa, B., T. Murray, and D. Rippin (2006), Active seismoelectric exploration of glaciers, *Geophys. Res. Lett.*, *33*, L07503, doi:10.1029/2006GL025758.

Martner, S. T., and N. R. Sparks (1959), The electroseismic effect, *Geophysics*, *24*(2), 297–308, doi:10.1190/1.1438585.

Mikhailov, O. V., W. M. Haartsen, and M. N. Toksöz (1997), Electroseismic investigation of the shallow subsurface: Field measurements and numerical modeling, *Geophysics*, *62*(1), 97–105, doi:10.1190/1.1444150.

Mikhailov, O. V., J. Queen, and M. N. Toksöz (2000), Using borehole electroseismic measurements to detect and characterize fractured (permeable) zones, *Geophysics*, *65*(4), 1098–1112, doi:10.1190/1.1444803.

Neev, J., and F. R. Yeatts (1989), Electrokinetic effects in fluid-saturated poroelastic media, *Phys. Rev. B*, *40*(13), 9135–9141, doi:10.1103/PhysRevB.40.9135.

Pride, S. R., and S. Garambois (2002), The role of Biot slow waves in electroseismic wave phenomena, *J. Acoust. Soc. Am.*, *111*(2), 697–706, doi:10.1121/1.1436066.

Pride, S. R., and S. Garambois (2005), Electroseismic wave theory of Frenkel and more recent developments, *J. Eng. Mech.*, *131*(9), 898–907, doi:10.1061/(ASCE)0733-9399(2005)131:9(898).

Pride, S., and M. W. Haartsen (1996), Electroseismic wave properties, *J. Acoust. Soc. Am.*, *100*(3), 1301–1315, doi:10.1121/1.416018.

Revil, A., P. A. Pezard, and P. W. J. Glover (1999), Streaming potential in porous media: 1. Theory of the zeta potential, *J. Geophys. Res.*, *104*, 20,021–20,031.

Russell, R. D., K. E. Butler, A. W. Kepic, and M. Maxwell (1997), Seismoelectric exploration, *Leading Edge*, *16*(11), 1611–1615, doi:10.1190/1.1437536.

Salama, R. B., R. Silberstein, and D. Pollock (2005), Soils characteristics of the Bassendean and Spearwood sands of the Gnangara mound (Western Australia) and their controls on recharge, water level patterns and solutes of the superficial aquifer, *Water Air Soil Pollut.*, *5*(1–2), 3–26, doi:10.1007/s11267-005-7396-8.

Singer, J., J. Saunders, L. Holloway, J. B. Stoll, C. Pain, W. Stuart-Bruges, and G. Mason (2006), Electrokinetic logging has the potential to measure permeability, *Petrophysics*, *47*(5), 427–441, Oct.

Strahser, M. H. P., W. Rabbel, and F. Schildknecht (2007), Polarisation and slowness of seismoelectric signals, a case study, *Near Surf. Geophys.*, *5*, 97–114.

Thompson, A. H., and G. A. Gist (1993), Geophysical applications of electrokinetic conversion, *Leading Edge*, *12*(12), 1169–1173, doi:10.1190/1.1436931.

Zhu, Z., M. N. Toksöz, and D. R. Burns (2008), Electroseismic and seismoelectric measurements of rock samples in a water tank, *Geophysics*, *73*(5), E153–E164, doi:10.1190/1.2952570.

K. E. Butler, Department of Geology, University of New Brunswick, P.O. Box 4400, Fredericton, NB E3B 5A3, Canada. (kbutler@unb.ca)

J. C. Dupuis, B. D. Harris, and A. W. Kepic, Department of Exploration Geophysics, Curtin University of Technology, GPO Box U 1987, Perth, WA 6845, Australia. (c.dupuis@curtin.edu.au; b.harris@curtin.edu.au; a.kepic@curtin.edu.au)